Deep Structures and Geodynamic Processes in the Present-Day Tien Shan

Kseniia Nepeina[1,✉], Elena Bataleva[1], Anatoly Rybin[1]

[1] Research Station of the Russian Academy of Sciences in Bishkek, Kyrgyzstan
✉ nepeina.k@mail.ru

Keywords: Tien Shan, geodynamic processes, geophysics, deep structures

1. Introduction

The Kyrgyz Tien Shan covers an area of intense intracontinental seismicity, for most earthquakes in southern Kyrgyz Tien Shan occur within the Indo-Eurasian convergence zone, and those in Eastern Kyrgyzstan mainly occur along major faults (Nikolaev line, Shamshi-Tunduk, Atbashi, Inylchek). The Tien Shan Orogeny occurred approximately 10 Ma (Jolivet, 2015). The upper-crust tectonic structures that formed during the intercontinental orogen of the Central Asian belt are of interest because existing modelling of these features is inaccurate and too general. Tracking of geological structures is key for robust geological reconstructions and geomechanical simulations, but distinction among individual crustal blocks is a complex task.

Many researchers, when isolating crustal blocks, rely on their definition by fault positions and offset. Geological and geophysical studies have been used to define the characteristics of the block structure of the Tien Shan (Brunet, McCann & Sobel, 2017; Umirova, Istekova & Modin, 2016; Rybin et al., 2015; Bielinski et al., 2003; Thompson et al., 2002). Previous works explain the state of the lithosphere beneath Tien Shan using the petrology and electrical conductivity of xenoliths (Batalev et al., 2011; Bagdassarov, Batalev & Egorova, 2011). Here, we use the geophysical technique called magnetotelluric soundings (MTS) to extend the study of geodynamic processes and geological block description with physical parameters. In this paper we show that the MTS approach is beneficial for the characterization of underground structures in the Earth's crust. Underground structures with different resistivity result in a distribution of electrical currents that can be measured with MTS soundings on the surface. This paper shows how the MTS technique can image geological structures up to 100 km depth as a geoelectric cross-section.

The record of annual geoelectric variation confirms a relationship with the underlying geodynamic processes in the Earth's crust (Bataleva, Rybin & Matiukov, 2019). The variations in geoelectric parameters are observed through geomagnetic measurements at geomagnetic stations or MTS profiles (Bataleva & Mukhamadeeva, 2018). It helps us to construct geophysical models of contemporary geodynamic processes. These contemporary geodynamic processes partly reflect the ongoing deformation of the orogenic system, specifically regional crust folding caused by the mountain-building mechanism.

2. Methods and techniques

The Research Station of the Russian Academy of Sciences (RS RAS) in Bishkek produces magnetotelluric sounding (MTS) profiles (Bataleva, Rybin & Matiukov, 2019; Bataleva & Mukhamadeeva, 2018). MTS is a technique for observations of the distribution of the geoelectric parameters of the Earth's crustal rocks. The physical signal source of the electromagnetic field is generated by variations due to heliospheric and terrestrial interactions in the magnetic field. For this reason, MTS observations are useful to link the electromagnetic parameter variations to the geodynamic processes. MTS data is useful to determine material properties and structure at depths greater than 5 km, as MTS inversion results delineate the nature of buried structures. The objective of this study is to use the MTS technique to identify the main crustal units (blocks, their boundaries, and basement horizons) in the Tien Shan region.

The presented cross-sections are the result of interpretation of MTS data. This procedure contains the starting and the resulting models. An inversion needs a 1D starting model, based on processed raw MTS data in MT-corrector software by North-West Ltd. (Zorin et al., 2020). Afterwards, we get apparent resistivity curves and impedance phases for the observation point. The starting model (Fig. 1b) of the geoelectric section contains in situ geological information, such as anomalies of the electromagnetic parameters (Przhiyalgovskii et al., 2018). The final model is a product of an iterative selection method after an automated inversion algorithm. We adjust the resulting model to ensure the best match between the observed and model curves of the apparent resistivity and impedance phases with the Tikhonov's regularizing function and its subsequent nonlinear minimization (Przhiyalgovskii et al., 2018; Berdichevsky et al., 2010). The numerical solution is a finite-element algorithm that allows the calculation of electromagnetic

DOI: 10.2312/yes19.04

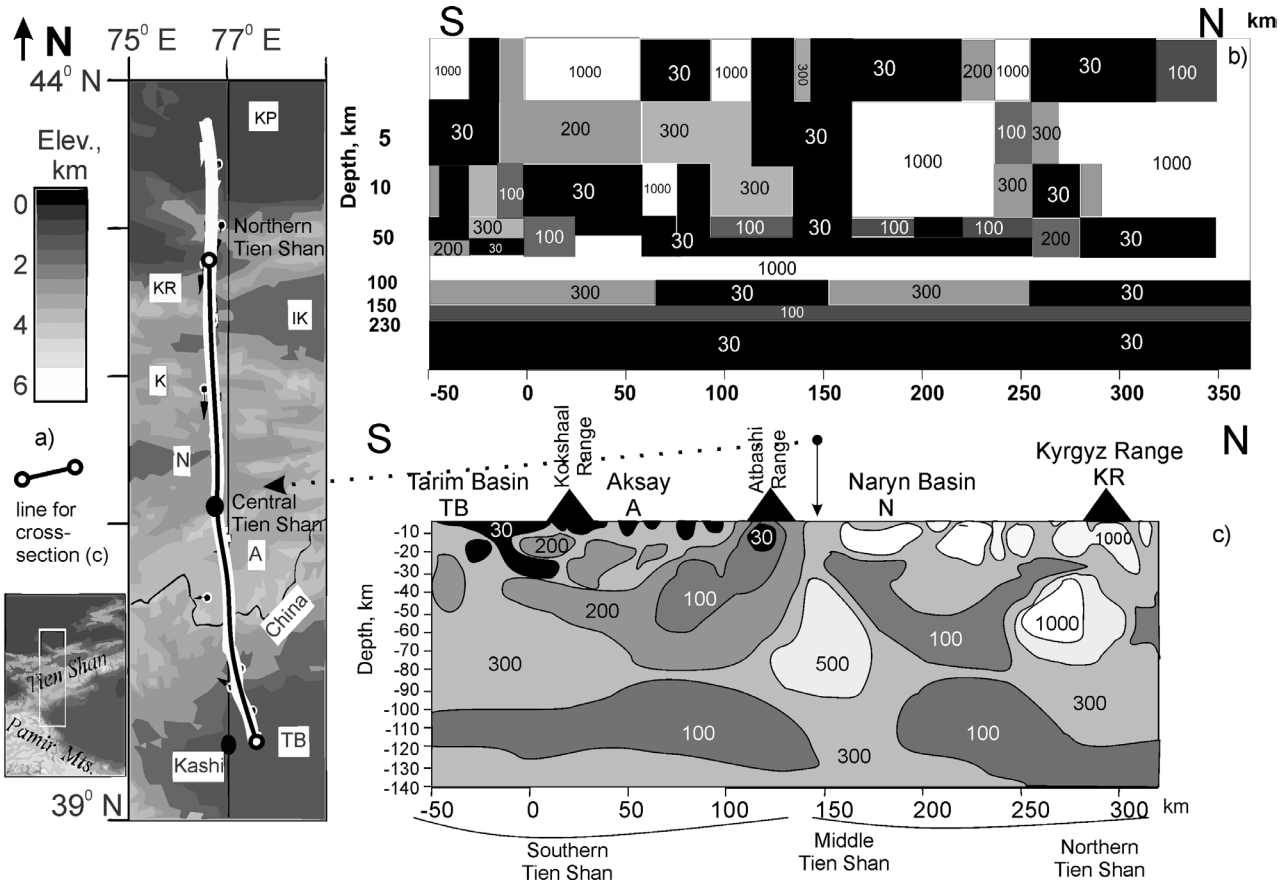

Figure 1: Map of the Tien Shan (MTS Naryn profile, 76° E) across the Kyrgyz Tien Shan and its' geoelectric cross-sections. (a) general map (after Bielinski et al., 2003); (b) geoelectric 1D starting model. Inside the model nodes the resistivity is indicated in Ohm·m (after Berdichevsky et al., 2010); (c) 2D inversion result model along the Naryn profile (adopted after Batalev et al., 2011). Inside the bodies, the resistivity is indicated in Ohm·m. Abbreviations: A - Aksay Basin; IK - Issyk-Kul; KR - Kyrgyz range; KP - Kazakh Platform; N - Naryn Basin; TB - Tarim Basin.

fields in 2D and 3D inhomogeneous media (Rodi and Mackie, 2001).

3. Results

The location of the interpretation of the Naryn profile (situated in the Tien Shan region along the 76° E meridian) is presented as Fig. 1a. Geoelectric models of the Naryn profile are shown in Fig. 1b and 1c. The starting 1D model is presented in Fig. 1b, a minimum block width of 25 km has been adopted (Fig. 1b).The final, interpretative model (Fig. 1c) presents the result of a 2D inversion with a simplified view. We restyled the cross-section view graphically using a rescaled boundary geometry of major bodies after Bielinski et al. (2003). Block structure is important during the profile construction to distinguish between areas of depressions and elevations.

We observe (Fig. 1c) in the southern part of the Naryn profile that the low-resistivity bodies extend in a horizontal plane at depths of at least 25 km. In the upper crust, there are relatively isometric isolated bodies that extend vertically. Objects with high resistivity values (> 500 Ohm·m) are mostly isometric and placed at 5 to 15 km depth in the Northern part of the profile.

Based on the distributions of geoelectric resistivity, we can conclude that the overall structure under the block of the Northern and the Middle Tien Shan (North of Atbashi Range, in Fig. 1c the right side from the central point with an arrow), adjacent to the Naryn depression, is significantly different from the Southern area (Fig. 1 c, left side). The difference suggests an essential 2D/3D heterogeneity. The Southern edge of the Naryn Basin, in connection with the Atbashi Range, has an area of increased resistivity (500 Ohm·m) below 35 to 40 km depth. On the west side, we observe more low-resistivity rock bodies – conductors (30 Ohm·m to 100 Ohm·m) – in the upper part of the cross-section (depths of 0 to 30 km). On the east side, we find high-resistivity rock bodies – dielectrics (600 to 1000 Ohm·m) – in the upper part of the cross-section (depths of 0 to 40 km). The anomalies in electric conductivity are revealed as sub-vertical conductors (30 to 200 Ohm·m) oriented along the flanks of the basins. The basement displays the resistivity values ≈ 200 to 300 Ohm·m.

Horizontal boundaries at depth correspond to the basement horizons, such as Moho (M), and vertical interfaces are clearly visible in the MTS cross-sections as resistivity contrast. We characterize the

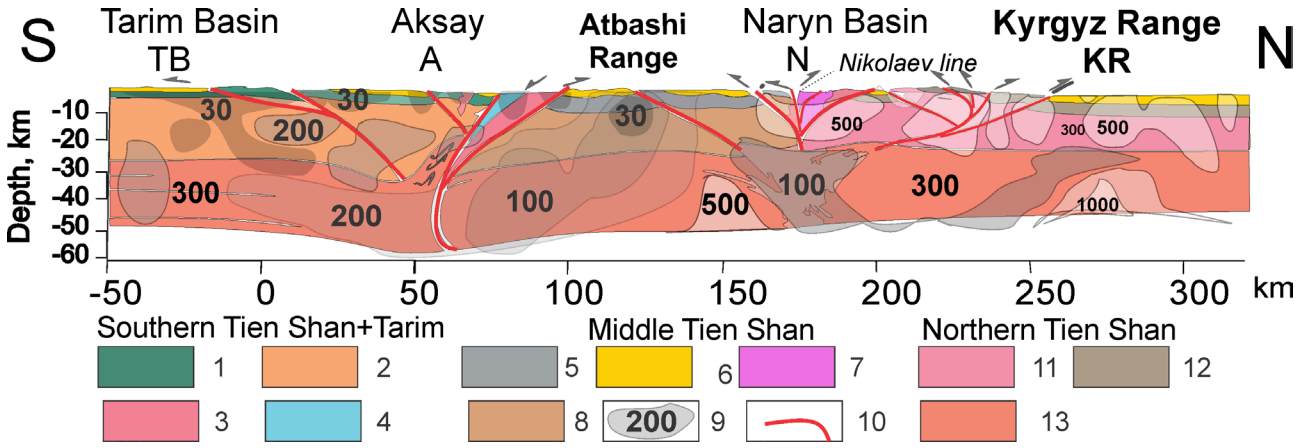

Figure 2: Interpretative crustal cross-section of the Tien Shan (Naryn profile) adopted after Jourdon et al. (2018), as the combination of the surface geological data (Przhiyalgovskii et al., 2018; Bataleva et al., 2017), thermo-mechanical model (presented in Jourdon et al., 2018) with the addition of geophysical data (restyled accordingly to results after Berdichevsky et al., 2010 and Bielinski et al. 2003). Legend: Southern Tien Shan: 1 - Paleozoic cover, 2 – Basement, 3- High pressure mica schists, 4 - Accretionary wedge; Middle Tien Shan: 5 - Paleozoic cover, 6 - Cenozoic cover, 7 - Permian granites, 8 – Basement; 9 – geoelectric bodies contours with apparent resistivity values, 10 – active faults (after Thompson et al., 2002); Northern Tien Shan: 11 – Ordovician plutons + basement, 12 – Paleozoic cover, 13 – Lower crust.

regional tectonics through the integration of our interpretation of the MTS profiles and in situ geologic studies (lithotypes, transversal faults, and crustal structures' geometry). We take into account geologic studies from Thompson et al. (2002) and Brunet, McCann, & Sobel (2017) for further interpretation.

The comparison (Fig. 2), adopted after Jourdon et al. (2018), shows the distinction between different parts of the Tien Shan. Overall in the Southern Tien Shan, the upper part of the sediment rock mass (Paleozoic cover) has resistivity values ≈ 30 to 50 Ohm·m. The lower crust below 30 km depth is about ≈ 300 to 500 Ohm·m with extensive dielectric areas (500 Ohm·m and above). The Naryn Basin is heavily compressed (Abdrakhmatov et al., 2001). In the upper part, we observe conductors (above 500 Ohm·m). The Atbashi Basin contains horizontal, slightly disturbed rocks at 0 to 10 km below the surface. The upper part at the Naryn Basin and Kyrgyz Ridge are distinguished with high resistivity values (500 to 1000 Ohm·m). The deep vertical areas at 30 to 50 km depth have the lowest-resistivity (100 Ohm·m). Moho (M) depths are taken from Vinnik et al. (2006). The Moho depth varies from 40 km in the North (Kyrgyz Range), up to 70 km in the South (near the Tarim Basin). The Moho geometry shows that the crust consists of isolated high resistivity bodies (> 1000 Ohm·m) separated by slightly more conductive zones.

4. Discussion

The Kyrgyz Tien Shan, in general, is defined as a 2-floor formation (the basement and the sediments). The basement is composed of volcanic-sedimentary and metamorphic rocks of Precambrian and Paleozoic age (Alexeiev et al., 2019). The Late Ordovician and Early Silurian granitoids penetrate the basement (Leonov et al., 2020). During the structural-geological mapping of various sections of the Northern and Middle Tien Shan, we acquired a material constitution and accurate description of disintegrated, clastic and weathered granites (Przhiyalgovskii et al., 2018; Rybin et al., 2018). Partially, unlike the host rocks, granites are intensely tectonized and have an extrusive nature (Przhiyalgovskii et al., 2018). Deformations of rocks are manifested in the form of various cataclasites (Bataleva et al., 2017), with most of them spread in brittle shear zones, especially in the upper parts of the crust. These zones are characterized by the products of dislocation metamorphism.

The difference in the left and right sides of Fig. 1b and 1c of the Naryn profile results from the different crustal architecture in the Southern and Northern Tien Shan. In the southern part of the Naryn profile, for example, we have interpreted low-resistivity bodies below 25 km depth to be the lower crust, and the presence of vertically isolated bodies in the upper crust suggests the fragmentation of the surface layer to a depth of 5 km. We date resistivity anomalies as the Permian granites in the upper Northern part of the profile. At the Naryn Basin and Kyrgyz Ridge, we have interpreted the near-surface bodies as granites with fragmentation. We consider they are cataclasites – a fine-grained, cohesive fault rock that forms dominantly by brittle deformation processes such as microcracking and abrasion. Sub-vertical conductive bodies may be controlled by the zones of the dynamic influence of faults and cataclasis of granite. At the Middle Tien Shan, the geologic bodies are folded as a "flower structure" and intersected by a series of faults

(Fig. 2), which were studied for the 76° E profile by Thompson et al. (2002). Moho depth variation is a result of the deformation of the crust in these regions.

Horizontal boundaries in the MTS cross-sections can be potentially associated either with faults, zones of deformation, zones of redistribution of matter, the presence of fluids, or with contrasts in rock formations and their chemical composition. We consider that the vertical areas with low resistivity (here termed 'conductor blocks') can potentially be saturated with fluids, and that these areas correlate only partially with surface faulting (as suggested by Thompson et al., 2002). This approach is partly confirmed in Bielinski et al. (2003), who suggested that these areas result from thrusting of a weaker crust of the Kyrgyz range southward over the strong crust of the Naryn block. According to these observations, it is possible to draw the vertical boundaries of blocks along gradient zones, where the dielectric blocks are separated from conductor blocks along of heterogeneity of conductivity.

5. Conclusions

We produce a geoelectric model for the Naryn profile. We interpret it on the basis of geologic features. We analyse our models and divide the Naryn profile into two parts, the southern and the northern, distinguished by geologic formation. The observed Moho depth is marked by high-resistivity anomalies and correlates with receiver function tomography results.

We investigate and explain the boundaries of blocks along gradient zones in geophysical results for geodynamic issues. We consider the low-resistivity layers below 25 km as the lower crust and prove the fragmentation of the surface layer in the southern part of the Naryn profile. Because the granites are disintegrated in the upper part of the profile, we assume deep saturation of the fluids.

The anomalies in electric conductivity help in rock state definition. Using MTS studies in the region, we clarify the variable degrees of the weathered, deformed, or water-saturated granite layers using low resistivity as an indicator for cataclasites. It means that they are broken with fractures. It proves a block structure at the meso-scale. The question of cataclastic fluid permeability is essential for earthquake modeling or looking for water- and fluid-bearing rocks.

6. Acknowledgements

This study is carried out with the support of the Russian Scientific Foundation under the project RSF No. 16-17-10059 "The relationship of tectonic and morphological characteristics of upper crust structures of intercontinental orogens between deep structure, minerageny and geological risks (on the example of the Tien Shan)". The authors are grateful to Nord-West Ltd. for MT-corrector software. We also acknowledge the editor, Dr. Fernández-Blanco, and anonymous reviewers for their comments, and Dr. Gunn and Dr. Fernández-Blanco for help improving the quality of the manuscript language.

7. References

Abdrakhmatov, K., R., Weldon, S., Thompson, D., Burbank, C., Rubin, M., Miller, M., Molnar, P. 2001. Origin, direction, and rate of modern compression of the central Tien Shan (Kyrgyzstan). Russian Geology and Geophysics. 10. pp. 1502–1526.

Alexeiev, D.V., Kröner, A., Kovach, V.P., Tretyakov, A.A., Rojas-Agramonte, Y., Degtyarev, K.E., Mikolaichuk, A. V., Wong, J., Kiselev, V. V. 2019. Evolution of Cambrian and Early Ordovician arcs in the Kyrgyz North Tianshan: Insights from U-Pb zircon ages and geochemical data. Gondwana Research 66. pp. 93–115. https://doi.org/10.1016/j.gr.2018.09.005.

Bagdassarov, N., Batalev, V., Egorova, V. 2011. State of lithosphere beneath Tien Shan from petrology and electrical conductivity of xenoliths. Journal of Geophysical Research. 116. B01202. https://doi.org/10.1029/2009JB007125.

Batalev, V.Y., Bataleva, E.A., Egorova, V.V., Matyukov, V.E. and Rybin, A.K. 2011. The lithospheric structure of the Central and Southern Tien Shan: MTS data correlated with petrology and laboratory studies of lower-crust and upper-mantle xenoliths. Russian Geology and Geophysics. 52(12). pp. 1592–1599. https://doi.org/10.1016/j.rgg.2011.11.005.

Bataleva, E., Rybin, A. and Matiukov, V. 2019. System for collecting, processing, visualization, and storage of the MT-monitoring data. Data. 4(3). https://doi.org/10.3390/data4030099.

Bataleva, E.A. and Mukhamadeeva, V.A. 2018. Complex electromagnetic monitoring of geodynamic processes in the Northern Tien Shan (Bishkek Geodynamic Test Area). Geodynamics & Tectonophysics. 9(2). pp. 461–487 (in Russian). https://doi.org/10.5800/GT-2018-9-2-0356.

Bataleva, E.A., Przhiyalgovskii, E.S., Batalev, V.Y., Lavrushina, E. V., Leonov, M.G., Matyukov, V.E. and Rybin, A.K. 2017. New data on the deep structure of the South Kochkor zone of concentrated deformation. Doklady Earth Sciences. 475(2). pp. 930–934. https://doi.org/10.1134/S1028334X1708013X.

Berdichevsky, M.N., Sokolova, E.Y., Varentsov, I.M., Rybin, A.K., Baglaenko, N. V., Batalev, V.Y., Golubtsova, N.S., Matyukov, V.E. and Pushkarev, P.Y. 2010. Geoelectric section of the Central Tien Shan: Analysis of magnetotelluric and magnetovariational responses along the Naryn geotraverse. Izvestiya, Physics of the Solid Earth. 46(8). pp. 679–697. https://doi.org/10.1134/S1069351310080057.

Bielinski, R.A., Park, S.K., Rybin, A., Batalev, V., Jun, S. and Sears, C. 2003. Lithospheric heterogeneity in the Kyrgyz Tien Shan imaged by magnetotelluric studies. Geophysical Research Letters. 30(15). 1806. https://doi.org/10.1029/2003GL017455.

Brunet, M.-F., McCann, T., Sobel, E.R. 2017. Geological Evolution of Central Asian Basins and the Western Tien Shan Range. Geological Society, London, Special Publications. 427. pp. 1–17. https://doi.org/10.1144/SP427.17.

Jourdon, A., Le Pourhiet L., Petit C., Rolland Y. 2018. The Deep Structure and Reactivation of the Kyrgyz Tien Shan: Modelling the Past to Better Constrain the Present. Tectonophysics. 746. pp. 530–548. https://doi.org/10.1016/j.tecto.2017.07.019.

Jolivet, M. 2015. Mesozoic tectonic and topographic evolution of Central Asia and Tibet: a preliminary synthesis. In: Brunet, M.-F., McCann, T., Sobel, E.R. Central Asian Basins And Tien Shan Range 13 Geological Evolution of Central Asian Basins and the Western Tien Shan Range. Geological Society, London, Special Publications. 427. pp. 19–55. https://doi.org/10.1144/SP427.2.

Leonov, M.G., Morozov, Y.A., Przhiyalgovskii, E.S., Rybin, A.K., Bakeev, R.A., Lavrushina, E.V., Stefanov, Y.P. 2020. Tectonic Evolution of the Basement–Sedimentary Cover System and Morh-

postructural Differentiation of Sedimentary Basins. Geotectonics. 54. pp. 147–172. https://doi.org/10.1134/S0016852120020089.
Przhiyalgovskii, E.S., Lavrushina, E. V., Batalev, V.Y., Bataleva, E.A., Leonov, M.G. and Rybin, A.K. 2018. Structure of the basement surface and sediments in the Kochkor basin (Tien Shan): geological and geophysical evidence. Russian Geology and Geophysics. 59(4). pp.335–350. https://doi.org/10.1016/j.rgg.2017.09.003.
Rodi, W. and Mackie, R.L. 2001. Nonlinear conjugate gradients algorithm for 2-D magnetotelluric inversion. Geophysics. 66(1). pp. 174–187. https://doi.org/10.1190/1.1444893.
Rybin, A.K., Bataleva, E.A., Morozov, Y.A., Leonov, M.G., Batalev, V.Y., Matyukov, V.E., Zabinyakova, O.B. and Nelin, V.O. 2018. Specific Features in the Deep Structure of the Naryn Basin–Baibichetoo Ridge–Atbashi Basin System: Evidence from the Complex of Geological and Geophysical Data. Doklady Earth Sciences. 479(2). pp. 499–502. https://doi.org/10.1134/S1028334X18040165.
Rybin, A.K., Pushkarev, P.Y., Palenov, A.Y., Ivanova, K.A., Mansurov, A.N. and Matyukov, V.E. 2015. New geophysical data on the depth structure of the Tien Shan intermontane depressions. Moscow University Geology Bulletin. 70(1). pp. 62–68. https://doi.org/10.3103/S0145875215110010.
Thompson, S.C., Weldon, R.J., Rubin, C.M., Abdrakhmatov, K., Molnar, P. and Berger, G.W. 2002. Late Quaternary slip rates across the central Tien Shan, Kyrgyzstan, Central Asia. Journal of Geophysical Research. 107(B9), 2203. https://doi.org/10.1029/2001JB000596.
Umirova, G.K., Istekova, S.A. and Modin, I.N. 2016. Using magnetotelluric sounding for estimation of oil-and-gas content of mesozoic era in Western Kazakhstan. Moscow University Bulletin. Series 4. Geology. 4, pp. 52–58 (in Russian). https://doi.org/10.33623/0579-9406-2016-4-52-58.
Vinnik, L.P., Aleshin, I.M., Kaban, M.K., Kiselev, S.G., Kosarev, G.L., Oreshin, S.I. and Reigber, C. 2006. Crust and mantle of the Tien Shan from data of the receiver function tomography. Izvestiya, Physics of the Solid Earth. 42(8). pp. 639–651. https://doi.org/10.1134/S1069351306080027.
Zorin, N., Aleksanova, E., Shimizu, H., Yakovlev, D. 2020. Validity of the dispersion relations in magnetotellurics: Part I—theory. Earth, Planets and Space. 72. 9. https://doi.org/10.1186/s40623-020-1133-4.